Supplementary information for

Identification of Mott insulators and Anderson insulators in self-assembled gold nanoparticles thin films

Cheng-Wei Jiang[1], *I-Chih Ni*[2], *Shien-Der Tzeng*[2], *Cen-Shawn Wu*[3] *and Watson Kuo*[1,*]

[1] Department of Physics, National Chung Hsing University, Taichung 402, Taiwan

[2] Department of Physics, National Dong Hwa University, Hualien 974, Taiwan

[3] Department of Physics, National Chang-Hua University of Education, ChangHua 500, Taiwan

*Corresponding author e-mail: wkuo@phys.nchu.edu.tw

I. Particle size and electrode design

Figure S1 shows the multilayer Au nanoparticle (NP) film deposited on the substrate with premade electrode. The gap between adjacent electrodes is 200 nm. The transmission electron microscopy image reveals that the synthesized AuNPs are highly uniform in size, having an average diameter of 12 nm.

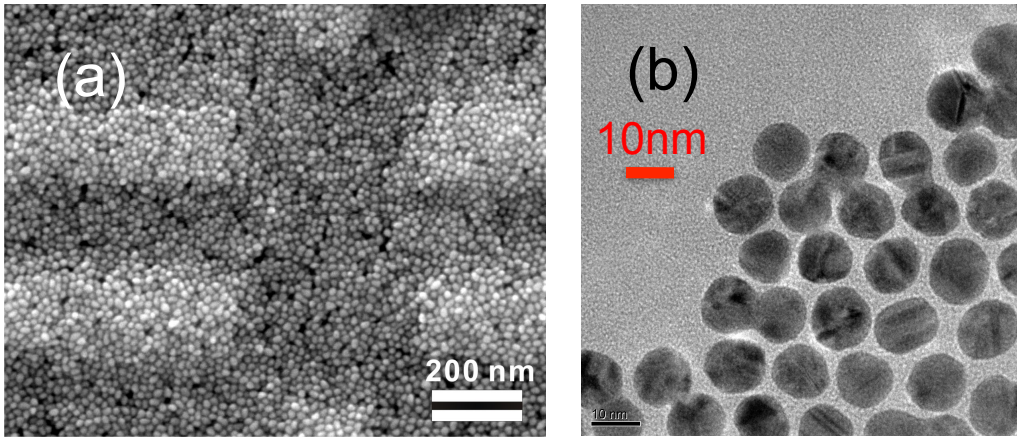

Figure S1 (a) The scanning electron micrographs of a multilayer MOA device. (b) The transmission electron microscopy image of the synthesized AuNPs deposited on a Si_3N_4 membrane. Here the capping molecules are MUA molecules.

Table I. Important parameters of the AuNPs devices deduced from data fitting described in the maintext.

	MUA	MOA	MHA	MPAii	MOAe	MPAi	MPAm
Carbon Number, n	11	8	6	3	8	3	3
Interparticle Spacing, s (nm)	1.88	1.51	1.27	0.90	1.51	0.90	0.90
R_{RT} (W)	10^7–10^9	~10^7	~10^6	10^5–10^6	10^1–10^7	~10^3	~10^3
T_1 (K)	43-80	40–52	45–56	32~49	17-50	<5	Metal
T_2 (K)	700-1600	500-780	460-860	573-770	6-210	6-9	
l(nm)	2.4-4.9	4.2-4.7	6.8-7.7	8.3-11			
κ	75-353	220-275	94-186	69-124			
E_C (meV)	11.0	9.3	8.1	6.0			
E_a(meV)	10.6-10.7	9.2	6.3-7.4	4.6-5.2			

II. Bending measurement

As described in the main text, we could measure the temperature dependent resistance when the substrate was bended. Such an experiment was realized by using a sample holder (Figure S2(b)) with brass chip supports (Figure S2(a)) of various surface curvatures. Their curvature radii are from 10 to 32 mm for convex ones and 3 mm to 7mm for concave ones. The chips were firmly attached to the support to keep the bending strain constant when varying temperature. Pogo pins were installed in the sample holder for a firmly connection between wiring and chip pads.

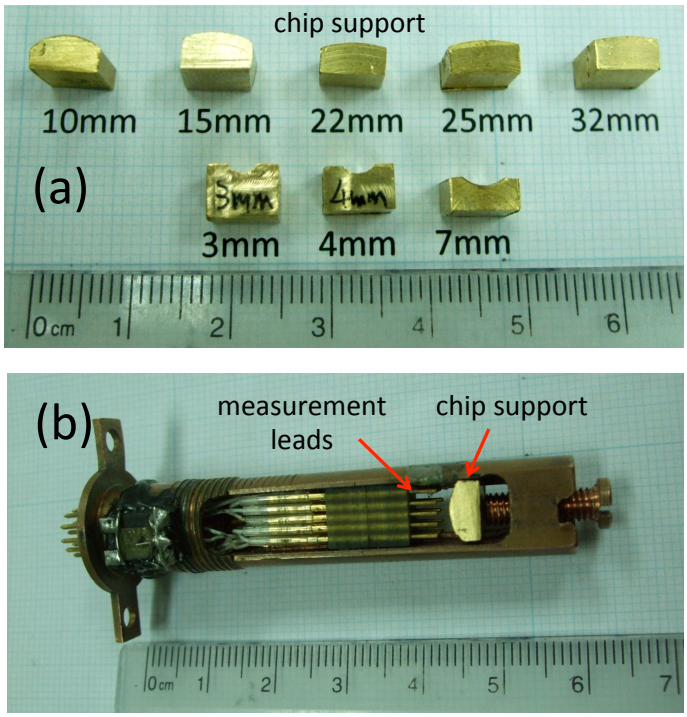

Figure S2 (a) Convex (top row) and concave (bottom row) chip supports made of brass for chip bending. The curvature radius is noted under each support. (b) The measurement sample holder with the cylindrical chip support.

III. Current-voltage characteristics of devices

The current-voltage(*IV*) characteristics of the metallic and insulating devices are qualitatively different: The metallic devices (MPA) showed linear *IV* curves when the temperature(*T*) was varied from 300 K to 10 K. On the other hand, insulating devices(MHA, MOA, and MUA) would show nonlinear *IV* curves when the temperature was lowered below 10 K. Furthermore, the resistance at zero-bias for metallic and insulating devices have opposite temperature dependences. For the metallic device, resistance reduces as *T* decreases, whereas for an insulating one, resistance increases several orders of magnitude as *T* decreases to 10 K.

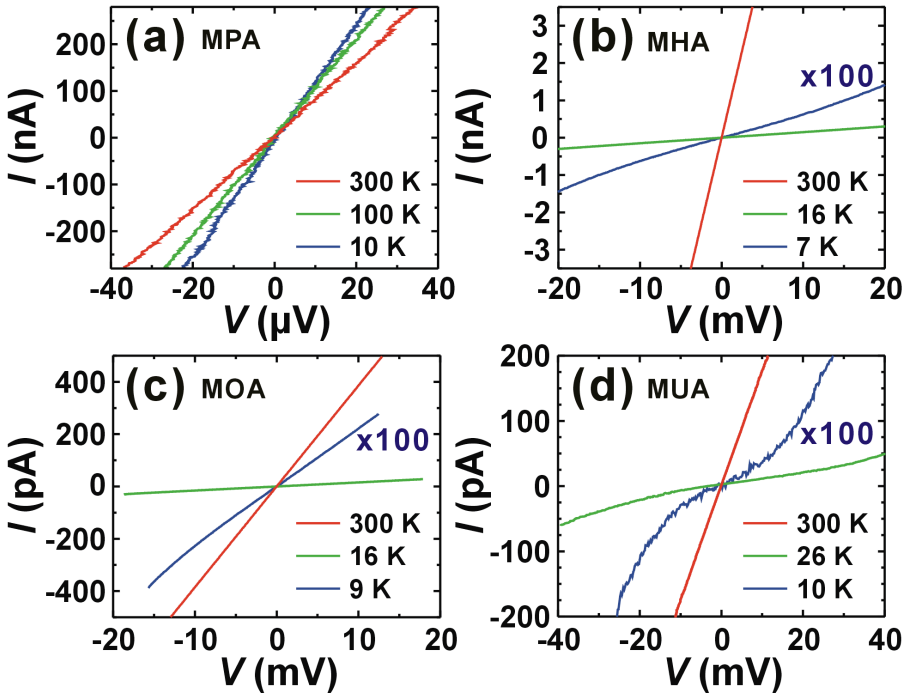

Figure S3 The *IV* characteristics for (a) MPAm, (b) MHA, (c) MOA, and (d) MUA devices. Clearly the insulating devices show non-linear *IV* curves at the base temperature. Notice that for clarity, the currents are amplified by 100 times for the base temperature (blue curves) cases in (b)-(d).

IV. Temperature dependent resistance

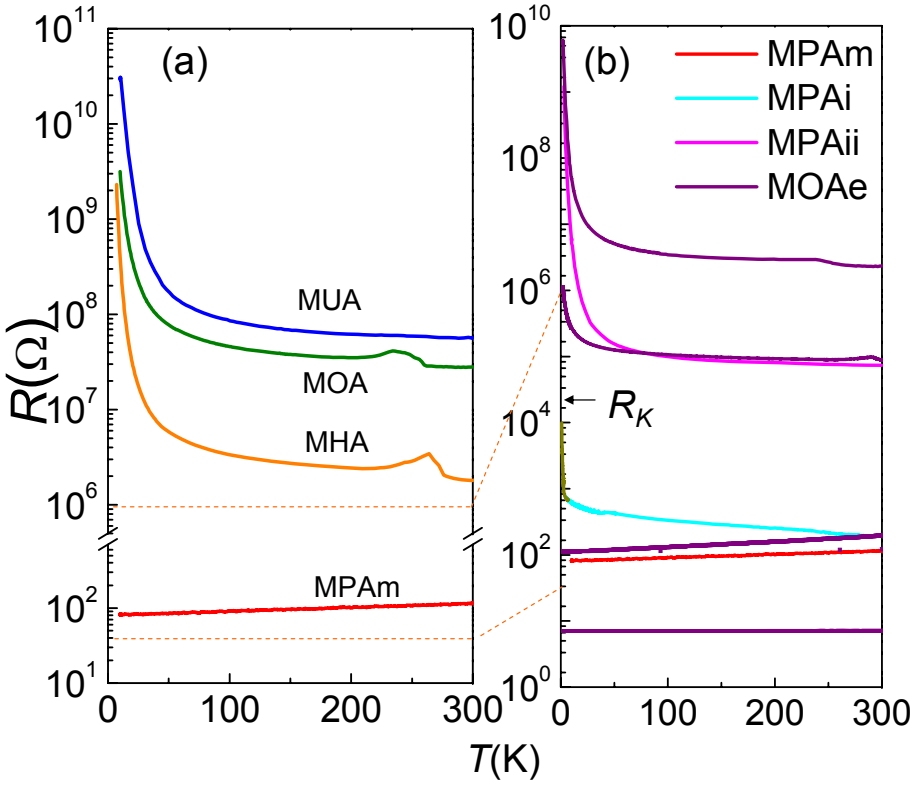

Figure S4 (a) The R vs. T curves for MUA, MOA, MHA and metallic MPA(MPAm) devices. The temperature dependence for the MPAm device shows a metallic behaviour while the others show insulating behaviours. For MOA and MHA devices, a small resistance hump is found at the temperatures around 235 K, which could be attributed to the contraction/expansion of residual water in the film. (b) $R(T)$ curves for various MPA and e-beam exposed MOA devices. The e-beam exposure reduces the tunnelling barrier height of the molecular junctions so as to reduce the room-temperature resistances of MOAe devices at most to 5 orders of magnitude, bringing low resistance devices (typically $R_{RT} < R_K$) across metal-insulator transition(MIT). NP assemblies linked by MPA molecules may have versatile $R(T)$ behaviours: When $R_{RT} > R_K$, the device is insulator(MPAii). When $R_{RT} < R_K$, it can be metallic (MPAm) or insulator (MPAi) possibly due to different strength of disorder. In addition to the interparticle coupling strength, the disorder, which is hardly determined by R_{RT}, serves as another parameter governing the MIT in these NP assemblies.

V. The temperature-dependent resistance of insulating devices

Here we show more R vs. $1/T$ plots for insulating devices. When T> 20 K, they follow the thermal activation property well.

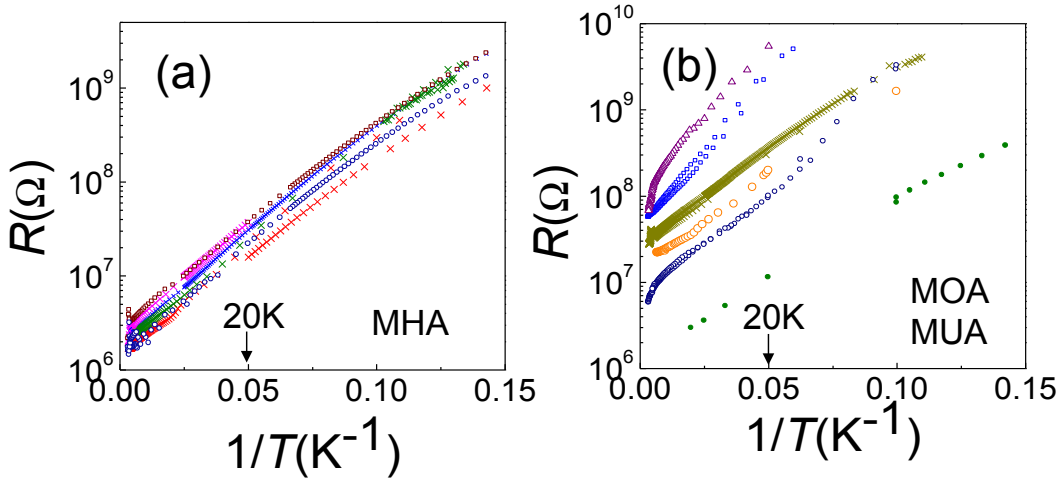

Figure S5 The R vs. $1/T$ plots for insulating MHA (a), MOA and MUA (b) devices. At higher temperatures, the resistance follows the thermal activation property, namely, $\ln R \propto T^{-1}$. Near room temperature, there is slight deviation, suggesting effect from thermal expansion.

VI. The co-tunneling and temperture-dependent resistance

As mentioned in the maintext, the the long-range charge hopping probability, from NP *i* to NP *j*, via the inelastic co-tunneling channel, is exponentially suppressed by the distance r_{ij},

$$\gamma_{ij} \propto \exp\left(-\frac{r_{ij}}{l_{in}}\right).$$

The localization length is temperature dependent,

$$l_{in} \sim \frac{2a}{\ln\left(E^2/16\pi k_B^2 T^2 g\right)}. \tag{1}$$

Here a is the average NP center–to-center distance, and g is the dimensionless conductance of the molecular junction. E is the average energy for electron and hole excitation energies, roughly on the order of E_a. The overall charge conduction should balance the charge hopping distance and energy cost, which arises from long-range Coulomb repulsion, $U \sim e^2/\kappa\varepsilon_0 r_{ij}$. κ is the effective dielectric constant of the NP assembly. Therefore the overall hopping probability should also include an Arrhenius factor, describing the thermal activation to overcome the energy U, and reads as

$$\gamma_{ij} \propto \exp\left(-\frac{r_{ij}}{l_{in}}\right)\exp\left(-\frac{e^2}{\kappa\varepsilon_0 r_{ij} k_B T}\right).$$

By maximizing γ_{ij} by varying r_{ij}, one obtain a most probable hopping range,

$$r^* \sim \sqrt{\frac{l_{in} e^2}{\kappa\varepsilon_0 k_B T}} \tag{2}$$

with the preferable hopping probability,

$$\gamma^* \propto \exp\left(-\frac{2r^*}{l_{in}}\right) = \exp\left(-2\sqrt{\frac{e^2}{\kappa\varepsilon_0 l_{in} k_B T}}\right). \tag{3}$$

In standard theory of Efros–Shklovskii(E-S) variable range hopping(VRH), the localization length is assumed constant of temperature to give a resistance as

$$R \propto \frac{1}{\gamma^*} \propto \exp\sqrt{\frac{T_2}{T}}\ .$$

On the other hand, in the case of the inelastic co-tunneling, one cannot neglect the temperature dependence in l_{in}. Yet this temperature dependence is weak so the resistance still follows the relation ln $R\sim T^{-1/2}$ well. To show this, we performed

calculation on the hopping exponent (r^*/l_{in}) in Eq. (3), using parameters obtained in our experiments. Here we used a=12 nm, g=0.01, $E/k_B(\sim T_1)$=50 K, κ=270. The blue curve is for temperature-dependent l_{in} using Eq. (1), while the green one is for temperature-independent one, in which l_{in} =0.1a is assumed. For a comparison, we also plot the function (r^*/l_{in}) =$(T_2/T)^{1/2}$ with T_2= 700 K as the red curve. As we have mentioned that Eq. (1) describes a slow varying function of T, the blue curve shows a nice linearity in this temperature regime. Moreover, all the curves have similar slope in this plot.

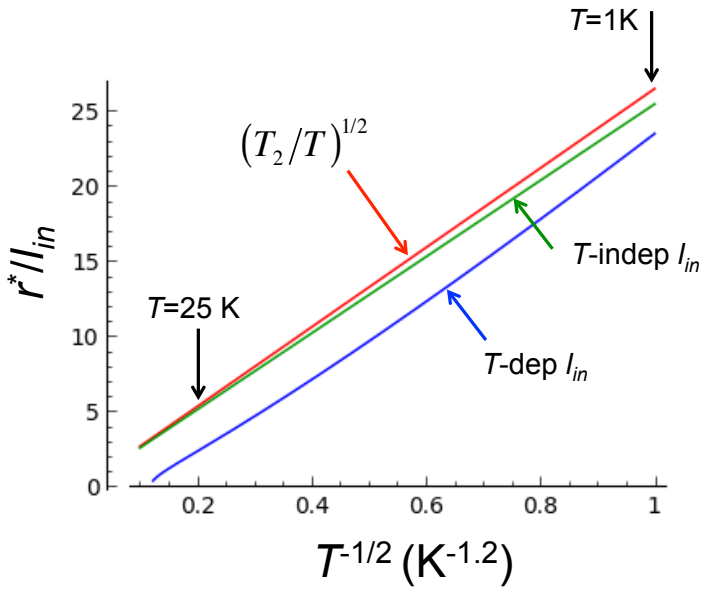

Figure S6 The exponent (r^*/l_{in}) vs. $T^{-1/2}$ plots for temperature-dependent l_{in} using Eq. (1) (blue), and temperature-independent l_{in} =0.1a (green). Both curves have very similar slope in this plot. The red curve plot the function (r^*/l_{in}) =$(T_2/T)^{1/2}$ with T_2= 700 K.

VII. Magnetoresistance

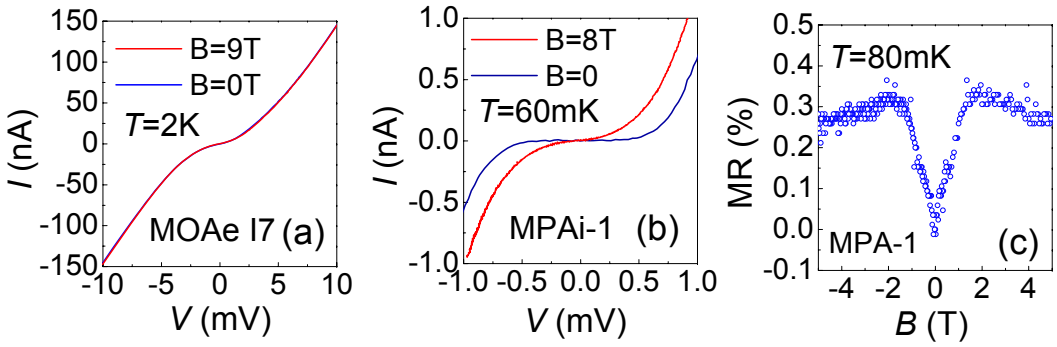

Figure S7 The repsonse of NP devices to a magnetic field. (a) Mott insulators(MOAe-I7) do not exhibit any magnetic field modulation at T=2 K. (b) MPAi Anderson insulators, can exhibit gate-modulated and magnetic field-modulated IV characteristics at a sufficiently low temperature. (c) MPA metallic devices present weak anti-localization. The field is parallel to the substrate.

VIII. The anisotropy of conduction under unidirectional strain

Accroding to WKB approximation, the interparticle tunnelling conductance exponentially decays with interparticle spacing, *s*, to yield $G_T \propto e^{-\beta s}$, in which β is related to the barrier height and electron mass. Expeirmental findings reveals that β is on the order of 10 nm^{-1} for most non-conducting molecules. When the substrate expands isotropically, the center-to-center distance, a of each nearest NP pair increases by a factor $(1+\varepsilon)$, in which ε is the strain. If the nanoparticle size is not changed in this expansion, the interparticle distance increases by $\Delta s = \varepsilon a$. This gives a (tunnelling) conductance change under isotropic expansion, $\Delta G_T / G_T \approx -\beta a \varepsilon$. In contrast to the isotropic expansion, a unidirectional strain would give different increment of interparticle spacing in different directions. Consider that the direction of interparticle tunnelling and of the strain have an angle θ(Figure S8). The projection of center-to-center length in the strain direction is $a_{\parallel} = a\cos\theta$. The stubstrate is elongated by a factor of 1+ε, while in the perpendicular direction the substrate is unchanged. Therefore the interparticle position vector becomes $a'_{\parallel} = a\cos\theta(1+\varepsilon)$ and $a'_{\perp} = a\sin\theta$. Again, assuming that *r* is not changed under the stress, one has

$$\begin{aligned}\Delta s &= \sqrt{a'^2_{\parallel} + a'^2_{\perp}} - a \\ &= \sqrt{a^2\cos^2\theta(1+\varepsilon)^2 + a^2\sin^2\theta} - a \\ &\simeq \cos^2\theta\varepsilon a\end{aligned} \quad .$$

Such a change in *s* should yield a conductance change $\Delta G_T / G_T \approx -\cos^2\theta\beta a\varepsilon$. When the tunnelling direction and the strain direction are the same, we have the maximal conductance change, $\Delta G_{T,p} / G_T \approx -\beta a\varepsilon$.

First we discuss the charging energy E_C of an AuNP in a NP network with strain. As described in the main text, the Abeles formula suggests that the charging energy is roughly proportional to the interparticle spacing, *s* when $r \gg s$. This suggests that the capacitance of constituent junction is inversely proportional to *s*. In a triangular lattice arrangement of the two-dimensional NP assembly, one NP can have 6 nearest neighbours to form 6 tunnel junctions. The total capacitance of these junctions with strain can be expressed as

$$\begin{aligned}C'_{\Sigma} &= \sum_{i=1}^{6} \frac{s}{s_i} C_0 = C_0 \sum_{i=1}^{6} \frac{1}{1+\varepsilon a s^{-1}\cos^2\theta_i} \\ &\simeq C_0 \sum_{i=1}^{6} \left(1 - \varepsilon a s^{-1}\cos^2\theta_i\right) = \left(1 - \frac{\varepsilon a}{2s}\right) C_{\Sigma}\end{aligned}$$

Here s_i is the interparticle spacing for *i*-th junction. C_0 is the capacitance for a tunnel

junction without strain and is considered as a constant, and the total capacitance of the tunnel junctions without strain should be $C_\Sigma = 6C_0$. The regular trianglar lattice gives $\sum_{i=1}^{6}\cos^2\theta_i = 3$. The changing energy is inversely proportional to C_Σ

$$E_C' = \left(1+\frac{\varepsilon a}{2s}\right)E_C = \left(1+\frac{1}{2\beta s}\frac{\Delta G_{T,p}}{G_T}\right)E_C \simeq \frac{2G_T+\Delta G_{T,p}}{2G_T}E_C = \frac{G_T+G_T'}{2G_T}E_C .$$

Here we used $\Delta G_{T,p}/G_T \approx -\beta a\varepsilon$, $\beta s \simeq (10\ \text{nm}^{-1})(0.9\ \text{nm}) \simeq 1$. This means that in the linear regime, an arithmetic average of conductance with strain(G_T') and without strain(G_T) could be a good estimation for the charging energy.

The quantum correction of Mott gap in general depends on the decay rate of a charge reside in a single NP. The decay rate, in general is proportional to the tunnelling conductance. To sum up all the decay rates to each neighbouring NP, Γ_i, we have

$$\Gamma_t' = \sum_{i=1}^{6}\frac{G_{T,i}}{G_T}\Gamma_0 = \Gamma_0\sum_{i=1}^{6}\left(1-\cos^2\theta_i\beta a\varepsilon\right) = \left(1-\frac{\beta a\varepsilon}{2}\right)\Gamma_t .$$

Here Γ_0 is the tunnelling rate between each NP pair wthout strain and is considered as a constant, and the decay rate without strain is $\Gamma_t = 6\Gamma_0$. Again, by noting the conductance measured along the strain direction as $G_T' \approx (1-\beta a\varepsilon)G_T$, one can express the decay rate as $\Gamma_t' = \frac{G_T+G_T'}{2G_T}\Gamma_t$. The arithmetic average of conductance with strain and without strain could also be an important parameter for the quantum fluctuation of charge.

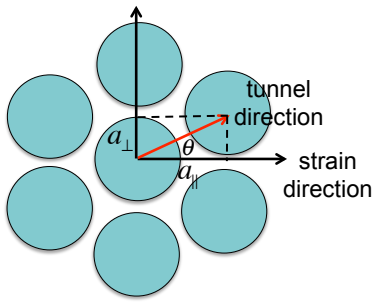

Figure S8 The triangular lattice of AuNP network.